Misalignment measurement of femtosecond electron bunches with THz repetition rate

J. Zhu,[1,2] E. Chiadroni,[3] R. Assmann,[1] M. Bellaveglia,[3] A. Cianchi,[4] M. Ferrario,[3] A. Giribono,[6,7] B. Marchetti,[1] A. Mostacci,[5] L. Piersanti,[3] R. Pompili,[3] and F. Villa[3]

[1]*Deutsches Elektronen-Synchrotron, DESY, Hamburg 22607, Germany*
[2]*Universität Hamburg, Hamburg 20146, Germany*
[3]*INFN-LNF, Via E. Fermi, 40-00044 Frascati, Rome, Italy*
[4]*University of Rome Tor Vergata and INFN, Via della Ricerca Scientifica, 00133 Rome, Italy*
[5]*University La Sapienza of Roma, via Antonio Scarpa 24, 00133 Roma, Italy*
[6]*Università degli studi di Roma "La Sapienza", P.le Aldo Moro 5, 00185 Roma, Italy*
[7]*INFN-Roma1, P.le Aldo Moro 5, 00185 Roma, Italy*

(Received 2 May 2016; published 26 April 2017)

Generation of a well-aligned bunch train is of vital importance for preserving the beam quality in a plasma wake-field accelerator. The simultaneous measurements of the relative misalignments in both planes, of the individual femtosecond electron bunches with THz repetition rate in a train, are reported and analyzed with simulations. The new method proposed in this paper demonstrates that the measurements can be done quickly by applying a single quadrupole scan together with a radio-frequency deflector (RFD), while the RFD strength and the RFD phase for each bunch do not need to be known.

DOI: 10.1103/PhysRevAccelBeams.20.042801

I. INTRODUCTION

An electron beam consisting of a train of short (∼100 fs scale) bunches, generated by combining laser pulse shaping and electron beam phase-space manipulation [1–4], has many attracting applications, e.g. two color free-electron laser (FEL) [5–7], THz radiation [8–9], superradiant radiation [10], and plasma wake-field acceleration (PWFA) [11–13].

In PWFA, a leading high-charge drive bunch (train) is used to excite fields in a plasma that in turn accelerate a trailing low-charge witness bunch. This technique offers the possibility for an affordable and compact high-energy collider as the plasma wave can sustain accelerating gradients several orders of magnitude higher than conventional accelerators. When a train of identical electron bunches separated by one plasma wavelength is matched into the plasma, the individual wake fields add up and the amplitude of the final wake field scales linearly with the number of bunches [14]. Furthermore, the transformer ratio (maximum energy gain of the witness bunch and maximum energy loss of the drive bunch) of the acceleration can be greatly enhanced when the bunch charge increases along the train [15].

Well-aligned beams are of vital importance for any kind of accelerators. In laser wake-field acceleration (LWFA), the misalignment of the bunch with respect to the laser beam will result in large emittance growth [16–17]. Similarly, the misalignment of the witness bunch with respect to the drive bunch (train) has the same effect in PWFA. Moreover, it is intuitive that the misalignments between the drive bunches will also affect the plasma wake-field generation, which in turn degrades the quality of the witness bunch.

Electromagnetic pickups [beam position monitors (BPMs)] serve as nondestructive beam diagnostic devices used in nearly any accelerator operating with bunched beams [18]. However, since the bandwidths of the pickup electrodes and the readout electronics are limited to several GHz nowadays, BPMs cannot discriminate between bunches with THz repetition rate. In this paper, a new method is proposed to simultaneously measure the relative misalignments of the individual femtosecond electron bunches with THz repetition rate in a train in both planes. The measurement is carried out by applying a single quadrupole scan together with a radio-frequency deflector (RFD). However, the RFD strength and the RFD phase for each bunch do not need to be known. We also present detailed analytical and simulation studies, which are crucial for understanding the influences from various jitter sources, particularly in the plane parallel to the deflecting voltage. The simulations and measurements agree very well, confirming the validity of this method.

II. EXPERIMENTAL SETUP

The experiments presented in the paper were carried out at the SPARC_LAB test facility [19]. The linac consists of a high brightness photoinjector, able to deliver electron beams from tens of femtoseconds to several picoseconds with energy up to 180 MeV. By illuminating the photocathode

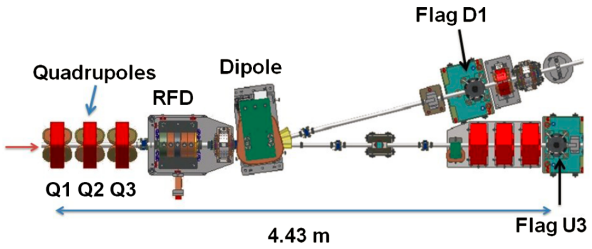

FIG. 1. Layout of the SPARC_LAB diagnostic section beam line. The beam is coming from the left side. The drawing is not to scale.

with a train of laser pulses and utilizing the velocity bunching technique [20–21], a train of femtosecond bunches with THz repetition rate can be generated [3] and fully characterized through transverse and longitudinal diagnostics measurements [22].

The diagnostics transfer line is sketched in Fig. 1, consisting of three quadrupole magnets followed by a vertical RFD (an S-band five-cell standing-wave rf deflecting cavity) [23] and a dipole magnet. The maximum power available for the RFD is approximately 2 MW. The view screen U3 is located 2.642 m downstream of the dipole center in the main beam line, and another view screen D1 is located 3.274 m downstream of the dipole magnet center in the 14° bending arm. Each of the view screens is composed of a piece of 100-μm-thick YAG:Ce crystal and normal to the respective beam line, with a 45° mirror placed on the back. The light is then collected by a 105 mm F11 lens and recorded with a Basler scout A640 CCD camera with pixel size of 7.4 μm (1∶3 magnification). The transverse emittance of the beam can be measured at U3 by the well-known quadrupole scan method [24] and the longitudinal phase-space of the beam can be measured at D1 by combining the RFD and the dipole magnet [25].

III. THEORY OF MISALIGNMENT MEASUREMENT

To first order, considering a beam line composed of nonskew quadrupole magnets, drifts, and a RFD streaking the beam in the vertical direction, the transverse coordinates of an electron at the screen are given by

$$x_f = R_{11}x + R_{12}x', \tag{1}$$

$$y_f \approx R_{33}y + R_{34}y' + B\phi, \tag{2}$$

where $[x, x', y, y']$ and $[x_f, y_f]$ are the initial and final transverse coordinates of the electron, respectively, R_{11}, R_{12}, R_{33}, and R_{34} are the transfer matrix elements between the initial and final locations with the RFD switched off, $B \approx eVR_{12}/pc$ [25] and φ (=0 for zero crossing) are the strength and the phase of the RFD, respectively, e is the electron charge, V is the equivalent deflecting voltage, p is the momentum of the electron and c is the speed of light in vacuum.

Since the energy spread of the concerned electron bunch is of the order of 10^{-3}, the misalignment of the bunch at the screen can be obtained by averaging Eqs. (1) and (2) on both sides,

$$c_{x_f} \approx R_{11}c_x + R_{12}c_{x'}, \tag{3}$$

$$c_{y_f} - Bc_\phi \approx R_{33}c_y + R_{34}c_{y'}, \tag{4}$$

where $[c_x,\ c_y]$ and $[c_{x_f},\ c_{y_f}]$ are the initial and final displacements of the bunch, respectively, $[c_{x'},\ c_{y'}]$ are the initial divergences of the bunch, and c_ϕ is the RFD phase for the centroid of the bunch. When the strength of a single quadrupole magnet is scanned, by measuring the final displacements of the bunch (on the screen at the flag U3), the displacements and divergences of the bunch at the initial location can be derived by linear regression using the vector forms of Eqs. (3) and (4):

$$\boldsymbol{c}_{x_f} \approx \boldsymbol{R}_{11}c_x + \boldsymbol{R}_{12}c_{x'}, \tag{5}$$

$$\boldsymbol{c}_{y_f} - Bc_\phi \approx \boldsymbol{R}_{33}c_y + \boldsymbol{R}_{34}c_{y'}. \tag{6}$$

Here we have assumed that $\boldsymbol{R}_{11}$ and $\boldsymbol{R}_{12}$ are linearly independent, as are $\boldsymbol{R}_{33}$ and $\boldsymbol{R}_{34}$.

The RFD amplitude and phase of each bunch are required in Eq. (6). However, because of the RFD phase and amplitude jitter as well as the bunch arrival-time jitter, it is impossible to measure the precise RFD phase and amplitude for each bunch. As we will be shown in the following, the jitter has a large impact on the measurement in the vertical plane. In order to avoid the measurements of the RFD voltage and the RFD phase for each bunch, Eq. (6) can be transformed into

$$\Delta\boldsymbol{c}_{y_f} \approx \Delta\boldsymbol{R}_{33}(c_y + \kappa c_{y'}), \tag{7}$$

where $\Delta\boldsymbol{c}_{y_f} = \boldsymbol{c}_{y_f} - \bar{c}_{y_f}$, $\Delta\boldsymbol{R}_{33} = \boldsymbol{R}_{33} - \bar{R}_{33}$, the upper bar indicates the average value during the quadrupole scan, and we have used the relationship $\Delta\boldsymbol{R}_{34} = \kappa\Delta\boldsymbol{R}_{33}$ [see the Appendix]. It is found that only $c_y + \kappa c_{y'}$ can be derived from Eq. (7). Under the condition of $\kappa c_{y'} \ll c_y$, the measured $c_y + \kappa c_{y'}$ is a good approximation to c_y. Considering that the initial location and the scanned quadruple magnet are connected by a drift space, their distance should be as short as possible since κ is simply the drift length.

After solving Eqs. (5) and (7) for every bunch in a train, the misalignment of each bunch with respect to the axis of the train can be calculated by weighting the corresponding bunch charge,

$$\hat{c}_{X,j} = c_{X,j} - \sum_j q_j c_{X,j}, \tag{8}$$

where q_j is the fractional charge of the jth bunch, X denotes any transverse coordinate, and the upper hat indicates the relative value.

In order to quantify the accuracy of the measurement, particularly in the vertical plane, we define the fractional measurement error for the transverse coordinate X as

$$h_X = \sqrt{\sum_j q_j(\hat{c}_{X,j} - \hat{c}_{X,j,in})^2 / \sum_j q_j \hat{c}^2_{X,j,in}}, \quad (9)$$

where $\hat{c}_{X,j,in}$ denotes the input relative misalignment of the jth bunch. The intrinsic error of the displacement measurement in the vertical plane is then given by

$$h_y = |\kappa| \sqrt{\sum_j q_j \hat{c}^2_{y',j,in} / \sum_j q_j \hat{c}^2_{y,j,in}}. \quad (10)$$

It is apparent that the accuracy of $\hat{c}_y$ improves as κ and $\hat{c}_{y'}$ decrease.

Understanding the influences of the RFD phase and voltage jitter is important to explain the measured data in the vertical plane. In the presence of jitter, Eq. (7) can be written as

$$\Delta \boldsymbol{c}_{y_f} = \Delta \boldsymbol{R}_{33}(c_y + \kappa c_{y'} + K) + \Delta \boldsymbol{J} - \Delta \boldsymbol{R}_{33} K, \quad (11)$$

where K is an additional effective value for the input displacement to represent the RFD jitter and $\Delta \boldsymbol{J} = \boldsymbol{J} - \bar{J}$ with $\boldsymbol{J}$ being the actual induced vertical displacements on the screen. The objective of the linear regression is to minimize the residual sum of squares, which is given by

$$\hat{\varepsilon} = (\Delta \boldsymbol{J} - \Delta \boldsymbol{R}_{33} K)^T (\Delta \boldsymbol{J} - \Delta \boldsymbol{R}_{33} K). \quad (12)$$

The minimum $\hat{\varepsilon}$ is achieved when the derivative of Eq. (12) with respect to K is zero, which gives

$$\begin{aligned} K &= \Delta \boldsymbol{J}^T \Delta \boldsymbol{R}_{33} / \Delta \boldsymbol{R}_{33}^T \Delta \boldsymbol{R}_{33} \\ &= \rho_{R_{33},J} \sigma_J / \sigma_{R_{33}}, \end{aligned} \quad (13)$$

where $\rho_{R_{33},J}$ is the Pearson's correlation coefficient between $\boldsymbol{R}_{33}$ and $\boldsymbol{J}$, and $\sigma_{R_{33}}$ and σ_J are the standard deviations of $\boldsymbol{R}_{33}$ and $\boldsymbol{J}$, respectively. Since $\sigma_{R_{33}}$ increases as the scan current range increases, K can be reduced by using a larger scan range.

In the presence of only the phase jitter, $\Delta \boldsymbol{J}$ is the same for each bunch in a train since each one has the same deflecting voltage increment. $\sigma_{R_{33}}$ and $\rho_{R_{33},J}$ are almost the same for each bunch as well since the energy differences between bunches are small. Consequently, K will be nearly the same for each bunch so that it can be eliminated in Eq. (8). Therefore, the phase jitter will basically not affect the measurement result.

In the presence of only the voltage jitter, since each bunch in a train has the same voltage jitter but a different phase, $\Delta \boldsymbol{J}$ is different for each bunch. However, $\rho_{R_{33},J}$ is still nearly the same for each bunch since the correlation has nothing to with the phase which is a constant for each bunch during the scan. Hence K will be different for each bunch so that it cannot be eliminated in Eq. (8). Therefore, the voltage jitter will introduce an error into the measurement result.

It should be pointed out that this method in principle ought to be used for relative misalignment measurement. In the horizontal plane, the fitted c_x and $c_{x'}$ will coincide with the absolute misalignment only if the horizontal position of the screen with respect to the accelerator axis has been calibrated. Otherwise, the fitted c_x and $c_{x'}$ will both be the real value plus a constant. For the relative misalignment measurement, the calibration is not necessary since this unknown constant will be eliminated in Eq. (8). While in the vertical plane, Eq. (8) is required to eliminate the RFD phase jitter. Nevertheless, the absolute misalignment of each bunch can be calculated straightforwardly by adding the misalignment of the whole bunch train measured by the BPM.

In addition, the energy of each bunch is required to calculate the transfer matrices from the initial location to the screen. Since the energy differences between bunches are expected to be less than 1%, the average energy of the train can be used to calculate the matrix for every bunch. In the following section, we will show that the result is not sensitive to the energy used in the calculation.

IV. SIMULATIONS

In order to validate the proposed method, the beam line used for the misalignment measurement was set up in ELEGANT [26]. The parameters of each bunch at the initial location, which is 0.2 m upstream of the center of Q1, are summarized in Table I. All the values are either measured or estimated from the experiment. The deflecting strength of the RFD is about 1.46 mm/ deg at the screen.

A. Simulations without any jitter

We first investigated the case without any jitter. The typical fits in both planes are shown in Fig. 2, which reveal

TABLE I. Summary of the input parameters for every bunch in the train used in the simulations. The parameters were chosen to be similar to the experimental working points. D1-D4 denote the drive bunches and W denotes the witness bunch. The centroid coordinates c_X are the values with respect to the accelerator axis, and t refers to the timing with respect to the zero crossing of the RFD.

	D1	D2	D3	D4	W
Q (pC)	54	58	48	45	20
β_x (m)	72	70	74	85	107
α_x	6.2	8.6	9.2	8.7	9.5
β_y (m)	60	82	92	74	85
α_y	−3.3	−2.6	−2.8	−3.2	−4.8
ε_x (μm)	3.0	3.4	3.3	3.3	1.7
ε_y (μm)	3.0	3.4	3.3	3.3	1.7
E (MeV)	104.68	104.61	104.59	104.66	104.75
$\Delta E_{\rm rms}/E$	0.0027	0.0032	0.0032	0.0034	0.0024
σ_t (fs)	82	69	62	58	53
t (ps)	−2.40	−0.96	0.35	2.03	3.86
c_x (μm)	−50	150	200	100	−100
$c_{x'}$ (μrad)	10	5	0	15	20
c_y (μm)	200	100	50	100	−100
$c_{y'}$ (μrad)	−10	20	15	0	10

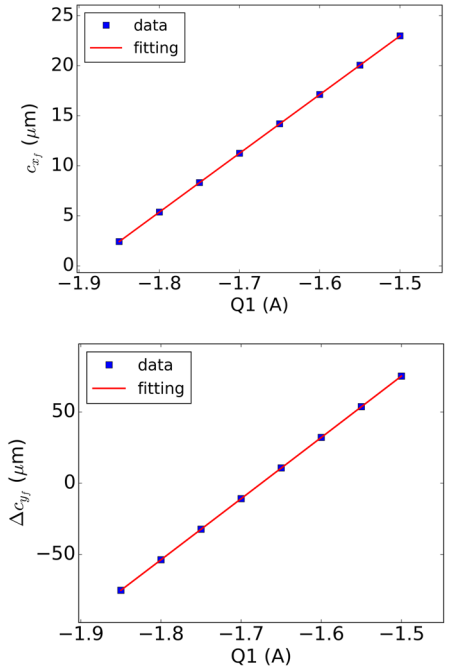

FIG. 2. Typical fits for a single bunch in both planes without any jitter.

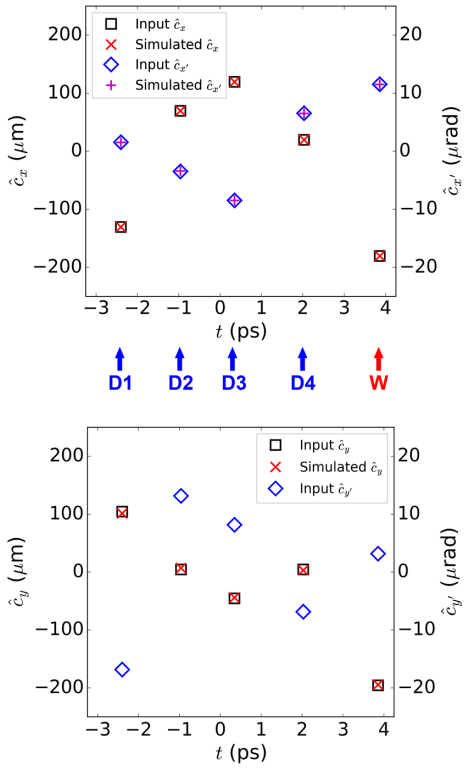

FIG. 3. Comparisons between the input and simulated misalignments in both planes without any jitter. The bunch train head is on the left. The inputs $\hat{c}_{y'}$ are also shown in the plot since they affect the accuracies of $\hat{c}_y$.

the linear relationship between the current of the quadrupole magnet and the bunch displacement on the screen. The input and simulated misalignments are compared in Fig. 3. It is found that the simulated displacements and divergences match the input precisely in the horizontal plane. In the vertical plane, the input and simulated displacements only slightly differ from each other.

For the simulation result shown in Fig. 3, h_y is about 0.03 ($\kappa \approx 0.20$). As a comparison, h_y will increase to about 0.14 ($\kappa \approx 0.97$) if Q3 is used for scanning instead of Q1. A small κ value is critical when the displacement is small. Considering that every c_y given in Table I is reduced by an order of magnitude, the measurement error will increase to 0.28 when Q1 is used for scanning. With an error of 0.28 the data can still correctly represent the relative displacements between bunches, as shown in Fig 4. In contrast, the error will become as high as 1.41 when Q3 is used for scanning, as shown in Fig. 5. Although we can still have a general knowledge of how good the relative misalignment is, the simulated relative vertical displacements between different bunches largely deviate from the input.

In practice, it is convenient to use an identical energy to calculate the transfer matrix for every bunch. Figure 6 shows the relationship between the measurement error and the energy used in the calculation. The reference energy is the average energy of the train. It is found that

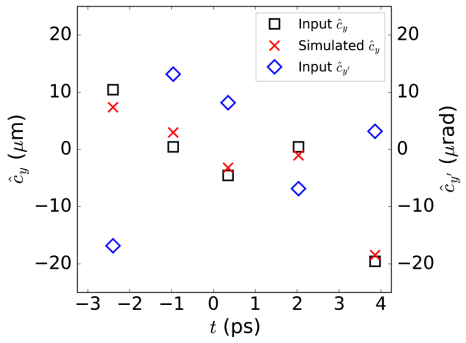

FIG. 4. Comparison between the input and simulated displacements in the vertical plane without any jitter. The input displacements are ten times smaller than those in Fig. 3. Q1 is used for scanning.

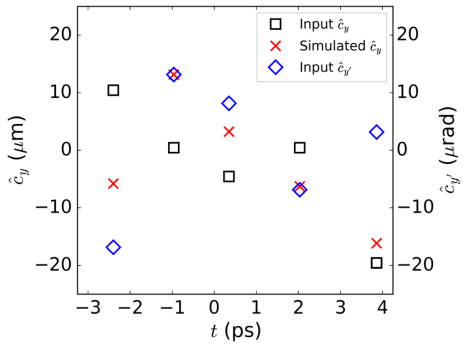

FIG. 5. Same as Fig. 4 but Q3 is used for scanning.

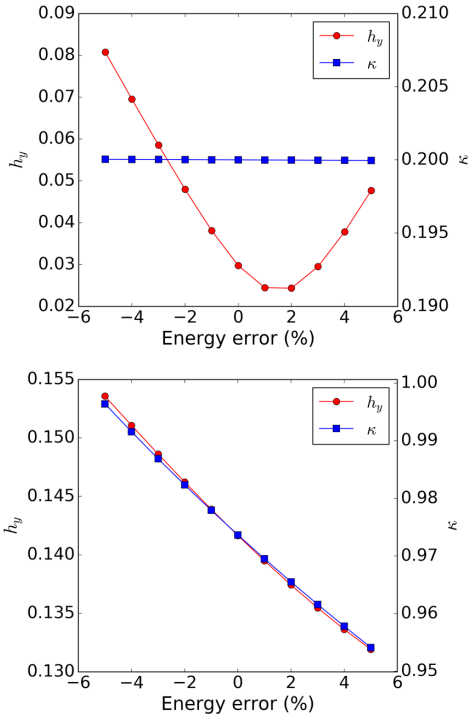

FIG. 6. Sensitivities of the measurement error to the energy used in the transfer matrix calculation. Top: Q1 is used for scanning. Bottom: Q3 is used for scanning.

the measurement error is not sensitive to the energy. When Q1 is used for scanning, the optimized energy is slightly larger than the average energy of the train. It is noteworthy that, when Q3 is used for scanning, the measurement error consistently decreases as the energy deviation increases. The decrease in the measurement error is mainly caused by the decrease in κ, which is mainly affected by the transfer matrices of Q1 and Q2.

B. Simulations with RFD jitter

The influences of the RFD voltage and phase jitter were demonstrated separately by 300 randomized simulations with a Gaussian distribution for each jitter source. In the simulation, the rms voltage and phase jitter were assumed to be 0.1% and 0.1°, respectively, which should be an overestimation for the S-band system nowadays [27]. The results are shown in Fig. 7. Consistent with the analytical study, the phase jitter does not increase the measurement error, while

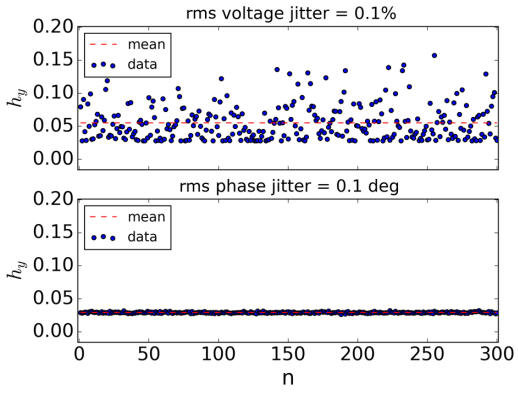

FIG. 7. Errors of the simulated vertical displacements with 300 random RFD voltages (rms jitter 0.1%) and phases (rms jitter 0.1°), respectively. Q1 is used for scanning.

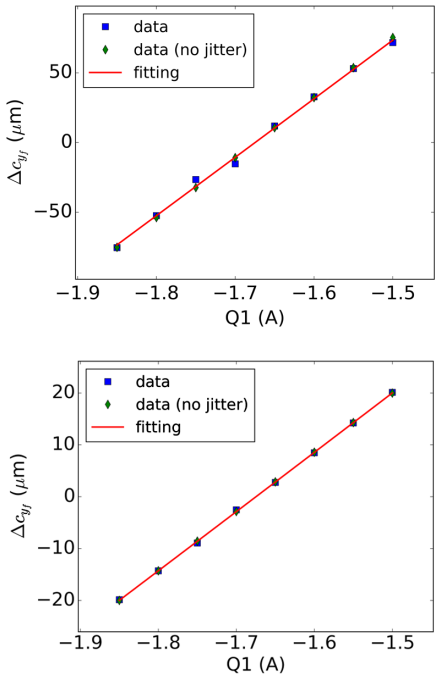

FIG. 8. Fits in the vertical plane for the first (top) and the third (bottom) bunches in the train. Only the RFD voltage jitter is included. The data points without any jitter are also plotted together for comparison.

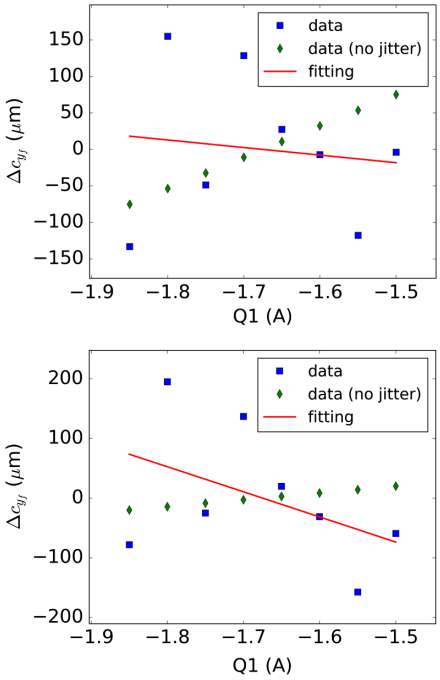

FIG. 9. Same as Fig. 8 except that only the RFD phase jitter is included.

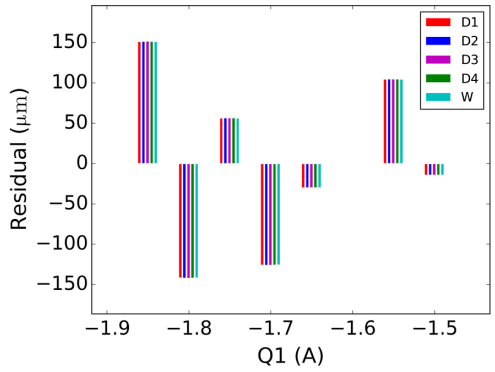

FIG. 10. Residuals for the fits with only the RFD phase jitter. The residual is defined as the difference between the predicted value and the data.

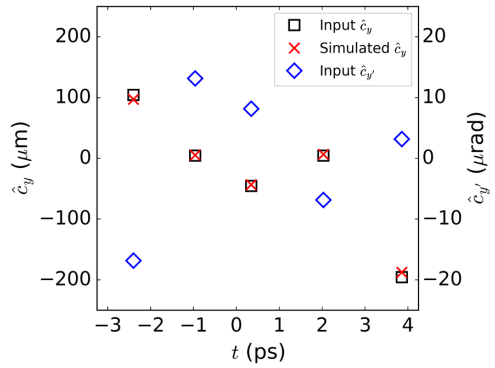

FIG. 11. Comparisons between the input and simulated misalignments in the vertical plane with both RFD phase and amplitude jitter included. Q1 is used for scanning.

the average error due to the voltage jitter increases to about 0.06 from 0.03. In addition, when Q3 is used for scanning, the average error increases to about 0.18 from 0.14 due to the voltage jitter. Simulations also confirm that the error growth halves when the current step increases from 0.05 A to 0.1 A.

The typical fits including jitter are shown in Figs. 8 and 9. The data points including only the voltage jitter slightly deviate from the fitted line when the RFD phase is not zero. However, the data points including only the phase jitter are widely scattered around the fitted line. It is noteworthy that these data points are always on the same side of the fitted line for each bunch at a given scan current, and the distances are almost the same as well, as shown in Fig. 10.

By combining the jitter used in the simulations shown in Figs. 8 and 9, the input and simulated misalignments with both RFD phase and amplitude jitter included are compared in Fig. 11. It indicates that the influence is almost negligible.

C. Simulations with beam position and pointing jitter

In real measurements, the initial misalignment of each bunch in a train jitters from shot to shot. The typical fits in the horizontal plane with an initial rms displacement jitter

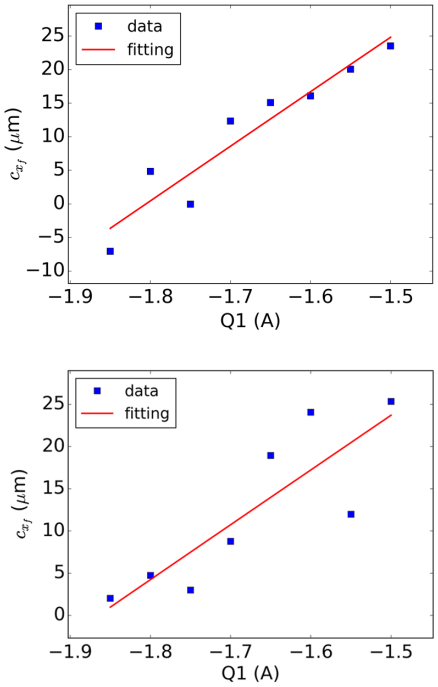

FIG. 12. Typical fits in the horizontal plane with an initial rms position jitter of 10 μm (top) and rms pointing jitter of 1 μrad (bottom).

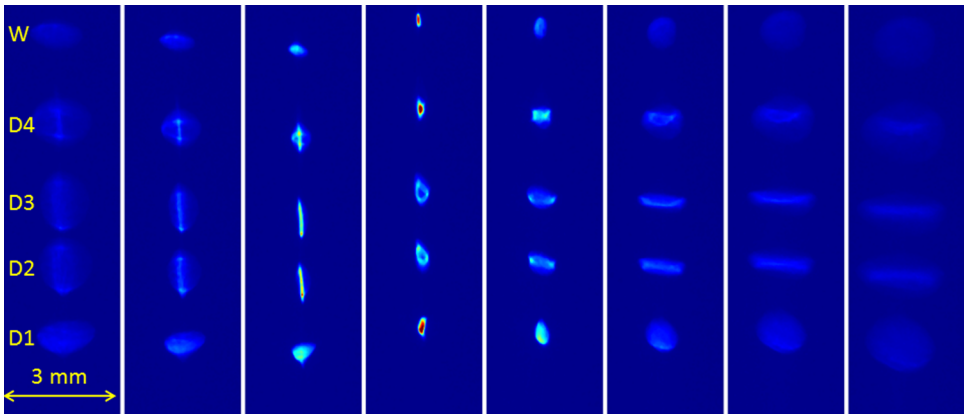

FIG. 13. Images of the bunch train on the screen (Flag U3) during the quadrupole scan from the No. 170652 experiment.

of 10 μm and divergence jitter of 1 μrad, respectively, are shown in Fig. 12. In principle, the position and pointing stabilities of each bunch can be inferred based on the experimental data in the horizontal plane, which are not affected by the RFD jitter. Similar to the RFD phase jitter, the correlated position and pointing jitter will not affect the relative misalignment measurement.

V. EXPERIMENTAL RESULTS

In the experiments, we measured the misalignment of each bunch in a train 0.2 m upstream of the center of Q1, where Q3 was used for scanning. Q3 was used instead of Q1 since we did not realize the difference between different scanning quadrupoles at that time. Ten images of the train were taken for each scan point and the average coordinates of the bunch centroid were calculated. The beam images for the No. 170652 experiment on the screen are shown in Fig. 13, and the fits for each bunch are shown in Fig. 14. The fractional charge of each bunch was calculated by weighting the intensity of the corresponding beamlet image.

We attribute the small scattering of the data in the horizontal plane to the position and pointing jitter of the

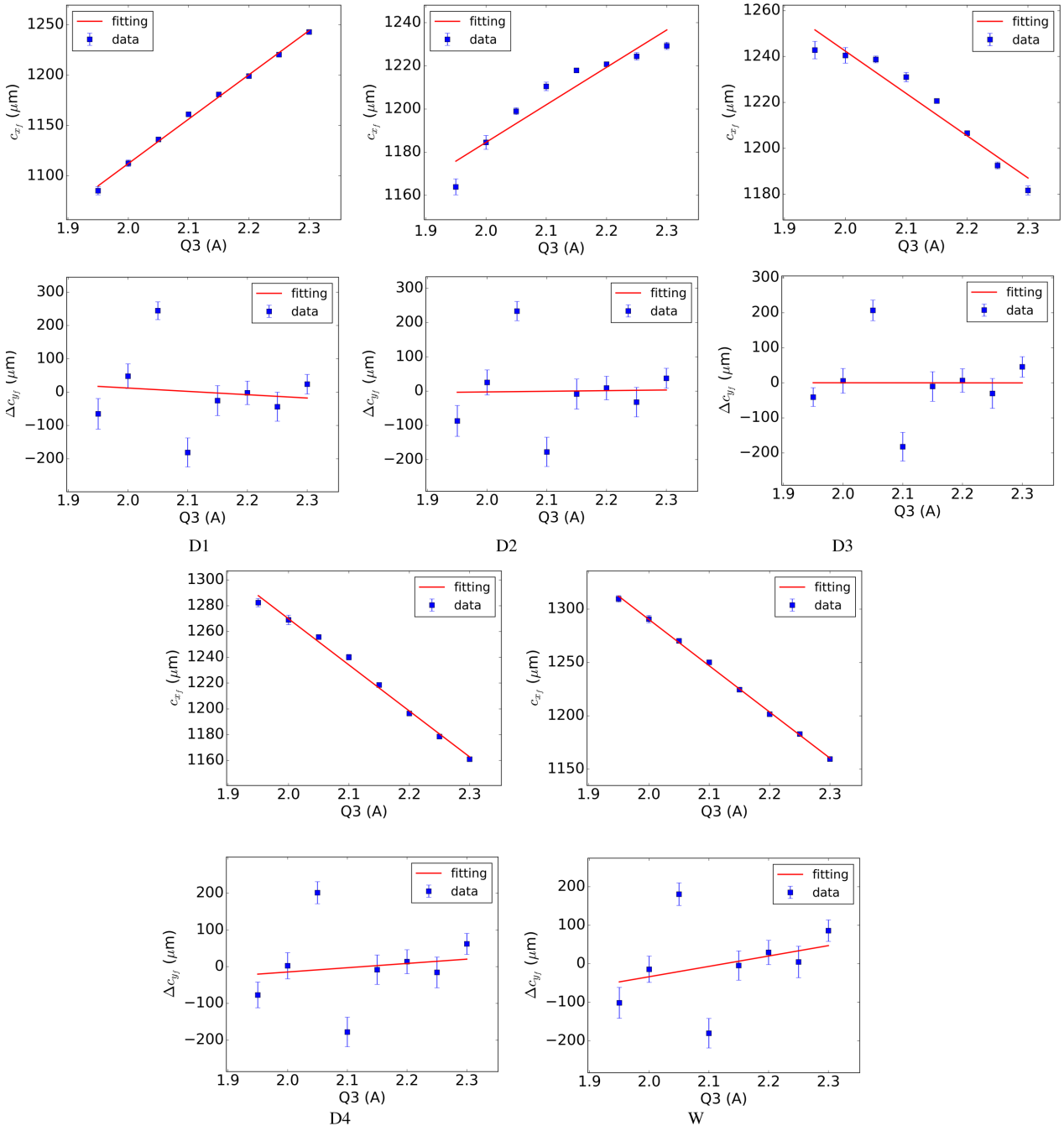

FIG. 14. Fits for each bunch in the train in the horizontal and vertical planes for the No. 170652 experiment.

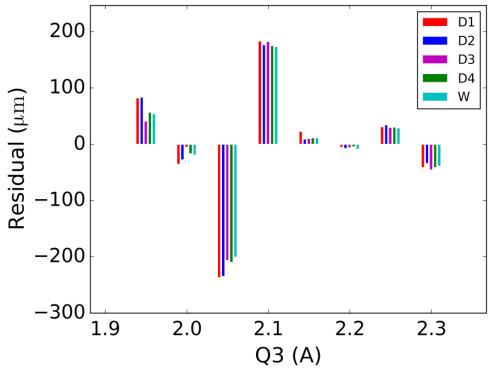

FIG. 15. Residuals for the fits in the vertical plane shown in Fig. 14.

incoming bunches, and the large scattering of the data in the vertical plane to the RFD phase jitter. It should be noted that the bunch arrival-time jitter will also contribute to the phase jitter. As shown in Fig. 15, the residuals of the fits are similar for each bunch at a given scan current. According to the previous analytical and simulation studies, this kind of jitter does not affect the relative misalignment measurement.

The relative misalignment of each bunch was then calculated and the results are shown in Fig. 16. Assuming the divergences of the individual bunches in the vertical plane are comparable to those in the horizontal plane, the average measurement error in the vertical plane

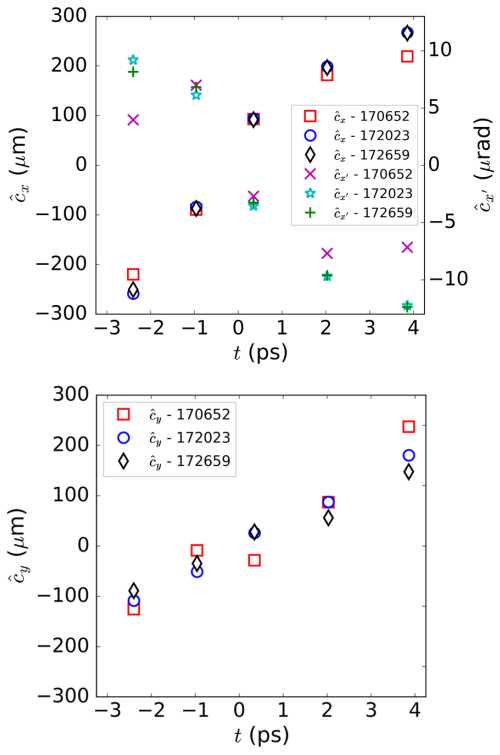

FIG. 16. Measured misalignments of each bunch in the train for the No. 170652, No. 172023, and No. 172659 experiments. The bunch train head is on the left.

is expected to be smaller than 0.25 without considering the misalignment jitter of the initial bunches. The measured bunch charge, energy, energy spread, bunch length, timing, horizontal emittance, and Twiss parameters for each bunch are the same as those listed in Table I.

The measured misalignments for another two experiments are also shown in Fig. 16. It is apparent that these results from different experiments are very similar. The displacements in both planes are also strongly correlated: they both increase monotonically from the bunch head to tail. Therefore, the misalignments were most likely induced by certain systematic errors during the generation or transportation of the bunch train.

VI. DISCUSSION AND SUMMARY

One possible explanation of the misalignments is the method used for generating the bunch train at the cathode. In these experiments, the bunch trains were produced by combining the properties of birefringent crystals and the flexibility of an interferometriclike configuration [28]. This scheme, which allows one to fully control and tailor the transverse, longitudinal, and energy characteristics of each pulse, however, requires a very good alignment in the transverse direction because of the transport optics (e.g. lenses) along the path towards the cathode. Any misalignment will change the relative transverse positions of the pulses over a long travel distance. Therefore, each bunch not only will experience a different energy because of the delayed injection phase but will also experience a different radial rf field in the gun because of the misaligned transverse arrival position on the cathode.

In this paper, we have demonstrated simultaneous measurement of the horizontal and vertical relative misalignments of the individual femtosecond electron bunches in a train with THz repetition rate by combining the single quadrupole scan method and a RFD. The challenge of the measurement lies in the plane parallel to the deflecting voltage, which was investigated both analytically and numerically. The largely scattered data in this plane, which will make the linear regression look very poor, was mainly induced by the RFD phase and bunch arrival-time jitter. However, the study proves that this kind of jitter has barely any influence on the relative misalignment measurement. The RFD voltage jitter, which only induces very small scattering of data, will introduce acceptable measurement error in the vertical plane. This additional error can be mitigated by using a large scan range of the current of the quadrupole magnet. Moreover, the setup between the initial location (where the misalignments are measured) and the scanned quadrupole magnet is important for reducing the measurement error in the vertical plane. In the case of a drift space, for instance, the length should be kept as short as possible. In addition, the average energy of the train can be used to calculate the transfer matrix for each bunch, and the result is not sensitive to this energy. The proposed misalignment measurement method is fast and

easy to implement, and the RFD strength and the RFD phase for each bunch do not need to be known. Finally, the absolute misalignment of each bunch can be calculated straightforwardly by adding the misalignment of the whole bunch train measured by the BPM.

APPENDIX: TRANSFER MATRIX

Under thin lens approximation, the transfer matrix between the initial position and the screen in the vertical plane is given by

$$\begin{aligned} R_V &= R_1 R_Q R_0 \\ &= \begin{bmatrix} a & b \\ c & d \end{bmatrix} \begin{bmatrix} 1 & 0 \\ q & 1 \end{bmatrix} \begin{bmatrix} e & f \\ g & h \end{bmatrix} \\ &= \begin{bmatrix} ae + bg + beq & af + bh + bfq \\ ce + dg + deq & cf + dh + dfq \end{bmatrix}, \end{aligned} \tag{A1}$$

where R_Q, R_0, and R_1 are the transfer matrices of the quadrupole magnet being scanned, and the beam line before and after this quadrupole magnet, respectively. It is obvious that

$$\kappa = \frac{\Delta R_{34}}{\Delta R_{33}} = \frac{R_{34} - \bar{R}_{34}}{R_{33} - \bar{R}_{33}} = \frac{f}{e}. \tag{A2}$$

[1] Y.-E. Sun, P. Piot, A. Johnson, A. H. Lumpkin, T. J. Maxwell, J. Ruan, and R. Thurman-Keup, Tunable Subpicosecond Electron-Bunch-Train Generation Using a Transverse-To-Longitudinal Phase-Space Exchange Technique, Phys. Rev. Lett. **105**, 234801 (2010).

[2] P. Muggli, V. Yakimenko, M. Babzien, E. Kallos, and K. P. Kusche, Generation of Trains of Electron Microbunches with Adjustable Subpicosecond Spacing, Phys. Rev. Lett. **101**, 054801 (2008).

[3] M. Boscolo, M. Ferrario, I. Boscolo, F. Castelli, and S. Cialdi, Generation of short THz bunch trains in a RF photoinjector, Nucl. Instrum. Methods Phys. Res., Sect. A **577**, 409 (2007).

[4] A. Mostacci *et al.*, in *Proceedings of the 2nd International Particle Accelerator Conference (IPAC11), San Sebastian, Spain* (EPS_AG, Spain, 2011), THYB01.

[5] A. A. Lutman, R. Coffee, Y. Ding, Z. Huang, J. Krzywinski, T. Maxwell, M. Messerschmidt, and H.-D. Nuhn, Experimental Demonstration of Femtosecond Two-Color X-Ray Free-Electron Lasers, Phys. Rev. Lett. **110**, 134801 (2013).

[6] V. Petrillo *et al.*, Observation of Time-Domain Modulation of Free-Electron-Laser Pulses by Multipeaked Electron-Energy Spectrum, Phys. Rev. Lett. **111**, 114802 (2013).

[7] C. Ronsivalle *et al.*, Large-bandwidth two-color free-electron laser driven by a comb-like electron beam, New J. Phys. **16**, 033018 (2014).

[8] Y. Shen, X. Yang, G. L. Carr, Y. Hidaka, J. B. Murphy, and X. Wang, Tunable Few-Cycle and Multicycle Coherent Terahertz Radiation from Relativistic Electrons, Phys. Rev. Lett. **107**, 204801 (2011).

[9] E. Chiadroni, M. Bellaveglia, P. Calvani, M. Castellano, L. Catani, A. Cianchi, G. Di Pirro, M. Ferrario, G. Gatti, O. Limaj, S. Lupi, B. Marchetti, A. Mostacci, E. Pace, L. Palumbo, C. Ronsivalle, R. Pompili, and C. Vaccarezza, Characterization of the THz radiation source at the Frascati linear accelerator, Rev. Sci. Instrum. **84**, 022703 (2013).

[10] A. Gover, Superradiant and stimulated-superradiant emission in prebunched electron-beam radiators. I. Formulation, Phys. Rev. ST Accel. Beams **8**, 030701 (2005).

[11] M. Litos *et al.*, High-efficiency acceleration of an electron beam in a plasma wakefield accelerator, Nature (London) **515**, 92 (2014).

[12] R. Pompili *et al.*, Beam manipulation with velocity bunching for PWFA applications, Nucl. Instrum. Methods Phys. Res., Sect. A **829**, 17 (2016).

[13] R. Assmann, R Bingham, T Bohl *et al.*, Proton-driven plasma wakefield acceleration: a path to the future of high-energy particle physics, Plasma Phys. Controlled Fusion **56**, 084013 (2014).

[14] E. Kallos, T. Katsouleas, P. Muggli *et al.*, in *Proceedings of the 22nd Particle Accelerator Conference (PAC07), Albuquerque, NM* (IEEE, New York, 2007), pp. 3070-3072, THPMS031.

[15] C. Jing, A. Kanareykin, J. G. Power, M. Conde, Z. Yusof, P. Schoessow, and W. Gai, Observation of Enhanced Transformer Ratio in Collinear Wakefield Acceleration, Phys. Rev. Lett. **98**, 144801 (2007).

[16] R. Assmann and K. Yokoya, Transverse beam dynamics in plasma-based linacs, Nucl. Instrum. Methods Phys. Res., Sect. A **410**, 544 (1998).

[17] I. Dornmair, K. Floettmann, and A. R. Maier, Emittance conservation by tailored focusing profiles in a plasma accelerator, Phys. Rev. ST Accel. Beams **18**, 041302 (2015).

[18] P. Forck, P. Kowina, and D. Liakin, *Beam Position Monitors*, CERN accelerator school on beam diagnostics (Le Normont, Dourdan, France, 2008), pp. 187–228.

[19] M. Ferrario, D. Alesini, M. Anania *et al.*, Emittance conservation by tailored focusing profiles in a plasma accelerator, Nucl. Instrum. Methods Phys. Res., Sect. B **309**, 183 (2013).

[20] L. Serafini and M. Ferrario, *AIP Conf. Ser.* 581, 87 (2001).

[21] M. Ferrario, D. Alesini, A. Bacci *et al.*, Experimental Demonstration of Emittance Compensation with Velocity Bunching, Phys. Rev. Lett. **104**, 054801 (2010).

[22] A. Cianchi, D. Alesini, and M. P. Anania, Six-dimensional measurements of trains of high brightness electron bunches, Phys. Rev. ST Accel. Beams **18**, 082804 (2015).

[23] D. Alesini, G. Di Pirro, L. Ficcadenti, A. Mostacci, L. Palumbo, J. Rosenzweig, and C. Vaccarezza, RF deflector design and measurements for the longitudinal and transverse phase space characterization at SPARC, Nucl. Instrum. Methods Phys. Res., Sect. A **568**, 488 (2006).

[24] H. Wiedemann, *Particle Accelerator Physics: Basic Principles and Linear Beam Dynamics* (Springer-Verlag, New York, 1993).

[25] P. Emma, J. Frisch, and P. Krejcik, SLAC Technical Report No. LCLS-TN-00-12, 2000.

[26] M. Borland, ELEGANT: A Flexible SDDS-Compliant Code for Accelerator Simulation, Advanced Photon Source LS-287 (unpublished).

[27] P. Craievich, S. Di Mitri, M. Milloch, G. Penco, and F. Rossi, Modeling and experimental study to identify arrival-time jitter sources in the presence of a magnetic chicane, Phys. Rev. ST Accel. Beams **16**, 090401 (2013).

[28] F. Villa, M. P. Anania, M. Bellaveglia, F. Bisesto, E. Chiadroni, A. Cianchi, A. Curcio, M. Galletti, D. DiGiovenale, G. DiPirro, M. Ferrario, G. Gatti, M. Moreno, M. Petrarca, R. Pompili, and C. Vaccarezza, Laser pulse shaping for high gradient accelerators, Nucl. Instrum. Methods Phys. Res., Sect. A **829**, 446 (2016).